crystals

MDPI

Article

Effect of Impurity Ions on Solubility and Metastable Zone Width of Lithium Metaborate Salts

Dan Li [1,2], Yong Ma [1,*], Lingzong Meng [1,2,*], Yafei Guo [2], Tianlong Deng [2] and Lan Yang [1]

[1] School of Chemistry and Chemical Engineering, Linyi University, Linyi 276000, China; lidan@lyu.edu.cn (D.L.); yanglan@lyu.edu.cn (L.Y.)

[2] Tianjin Key Laboratory of Marine Resources and Chemistry, College of Chemical Engineering and Materials Science, Tianjin University of Science and Technology, Tianjin 300457, China; guoyafei@tust.edu.cn (Y.G.); tldeng@tust.edu.cn (T.D.)

* Correspondence: mayongboy76@126.com (Y.M.); menglingzong@lyu.edu.cn (L.M.); Tel./Fax: +86-539-7258620 (Y.M.)

Received: 12 February 2019; Accepted: 26 March 2019; Published: 29 March 2019

check for updates

Abstract: The metastable zone width (MZW) of lithium metaborate salts at various concentrations was determined using the laser technique. The solubility data for lithium metaborate salts was nearly the same in the presence of NaCl at various concentrations. The MZW of lithium metaborate salts decreased when the stirring rate increased, but increased remarkably with increasing cooling rates and an increasing concentration of sodium chloride. The apparent secondary nucleation order for lithium metaborate salts was obtained using the Nývlt's approach. The apparent secondary nucleation order *m* of lithium metaborate salts is 4.00 in a pure $LiBO_2-H_2O$ system with an improved linear regression method. The *m* for lithium metaborate salts was enlarged in the system $LiBO_2-NaCl-H_2O$.

Keywords: solubility; metastable zone width; lithium metaborate salts; nucleation order

1. Introduction

Various borates are widely used in various industries such as nonlinear optical material, fluorescent material, and laser crystal material. The salt lake brines distributed in Qaidam Basinare rich in lithium and boron resources [1]. Borate is hard to crystallize out, but accumulate in the highly concentrated brine during the brine evaporation [2]. The borate usually has an obvious metastable phenomenon because there are many polyborate ions in the borate solution [3]. Lithium metaborate salt crystallizes from the tetraborate solution during the brine evaporation at a low temperature [4], but lithium tetraborate does not crystallize from the tetraborate solution. Therefore, it is meaningful to study the metastable zone width (MZW) of lithium metaborate salt for its comprehensive utilization of boron resources.

The metastable zone of salts was influenced with the dissolution temperature, stirring intensity, cooling rate, impurities, and more [5–13]. The MZW of boric acid, borax decahydrate, and potassium tetraborate tetrahydrate have been investigated in many research studies [8–13], but the metastable zone width of lithium metaborate salts were not been studied in the literature. The univalent ions (Na^+) narrow the metastable zone of H_3BO_3, while bivalent ions (Mg^{2+}, Ca^{2+}) broaden it [9,10]. For borax decahydrate, the MZW decreased with KCl in the solution [11]. The variation tendency of MZW varies with the impurity concentrations. A noticeable widening of the MZW was found after adding Cl^- and $SO_4{}^{2-}$ impurities to the solution [12]. The MZW of $K_2B_4O_7{\cdot}4H_2O$ decreases with the impurity concentration (Li^+, Ca^{2+}) increasing [13]. The results show that the MZW of a different borate is very different. In this paper, the laser intensity technique was applied to measure the MZW of lithium metaborate salts both in pure and NaCl solutions.

2. Experimental Section

2.1. Materials and Apparatus

The lithium metaborate with purities of ≥0.999 (in mass fraction) and sodium chloride with purities of ≥0.995 supplied from Aladdin Industrial Corporation (Shanghai, China) were used in the experiments, without any further purification. The experimental equipment for determining the metastable zone width was listed in Figure 1. The glass crystallizer was a triple jacketed vessel with the volume of 250 mL and internal diameter of 70 mm. A thermostatic bath from Jintan Guowang Experimental Instrument Factory (Jintan, China) (THD-2006, temperature uncertainty ±0.1 K) was applied to control the temperature of the crystallizer. The laser apparatus (GZ-2A, Beijing TuoDa Laser Instrument Co., Ltd. Beijing, China) detected nucleation/dissolution by emitting a light with a wave length of 632.8 nm into the crystallizer with the solution. The solubilities were measured in a multi-point magnetic stirring thermostatic bath (HXC-500-4A, Changzhou Nuke Instrument Co. Ltd., Changzhou, China, temperature precision ±0.1 K). The solid phases were identified with an Expert PRO X-ray diffractometer (XRD) from Spectris. Pte. Ltd., Almelo, The Netherlands.

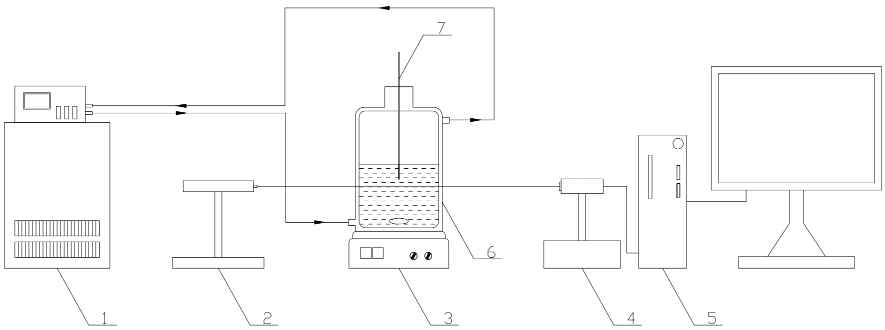

Figure 1. For metastable zone width experiments. 1. Thermostatic bath. 2. Laser generator. 3. Electromagnetic stirrer. 4. Photoelectric converter. 5. Numerical indicator. 6. Jacketed glass vessel. 7. Precise thermometer.

2.2. Experimental Method

The solutions saturated with lithium metaborate salts were obtained with the isothermal dissolution method [14]. The artificial synthesized brines were mixed with some salts and double distilled water. The glass bottles with synthesized brine sand were placed in the magnetic stirring thermostatic bath to obtain the equilibrium of those brines. The clarified solutions in each bottle were taken out for chemical analysis at least two times. If the relative error among the solution contractions from the same bottle was less than 0.3%, the equilibrium solution saturated with undissolved salts can be obtained. The solid phases were also separated from the solution for the identification with XRD. The saturated solution was used to measure the MZW of lithium metaborate salt.

The MZW of lithium metaborate salt in double distilled water (DDW) and the solution with sodium chloride was measured with the laser transmission method [11]. The saturated solution with the volume about 180 mL obtained with the isothermal dissolution method was placed into the crystallizer. The solution was cooled with the settled cooling rate until the first visible nucleus appears. The temperature when lithium metaborate salt crystallized was recorded with T_{nuc}. ΔT_{max} calculated with T_{nuc} and the saturation temperature (T_{sat}) with Equation (1) is considered as the MZW. The experiments were carried out at four constant cooling rates of (6.0, 9.0, 12.0, and 18.0) K·h^{-1} and a constant stirring rate, but at various saturated solutions. The experiments were run about three times to ensure the accuracy of the results. The results of MZW shown in this study were the average data.

$$\Delta T_{max} = T_{sat} - T_{nuc} \tag{1}$$

2.3. Analysis Method

The Cl^- ion concentration was analyzed by titration using an $Hg(NO_3)_2$ standard solution with diphenyl carbazone and bromophenol blue as the indicator [15]. The boron concentration was analyzed with the modified mass titration method using NaOH standard solution in the presence of mixture indicators of methyl red plus phenolphthalein and excessive mannitol conditions [15]. The relative error for titration among three parallel samples was no more than 0.003 in mass fraction. The standard uncertainties u_w for NaCl and $LiBO_2$, which were calculated with the boron and chlorine ion concentrations of 0.0049 and 0.0035, respectively.

3. Results and Discussion

3.1. Solubility for Systems $LiBO_2-H_2O$ and $LiBO_2-NaCl-H_2O$

The solubility for systems $LiBO_2-H_2O$ and $LiBO_2-NaCl-H_2O$ were studied and shown in Table 1. The mass fraction w expressed the concentration of the solution. The solubility for the $LiBO_2-H_2O$ system at 303.15 K, 313.15 K, and 323.15 K were compared with the data from the literature [16], which was shown in Figure 2. The experimental results in this study agree well with the data from the literature [16]. The results in Figure 2 illustrate that the experimental method and analysis in this work are credible.

Table 1. Experimental solubility data in the systems $LiBO_2-H_2O$ and $LiBO_2-NaCl-H_2O$.

No.	Liquid Phase, 100w		T/K	Equilibrium Solid Phase
	$LiBO_2$	NaCl		
1	4.88	0.00	303.15	$LiBO_2 \cdot 8H_2O$
2	7.43	0.00	313.15	$LiBO_2 \cdot 2H_2O$
3	7.93	0.00	323.15	$LiBO_2 \cdot 2H_2O$
4	4.97	4.47	303.15	$LiBO_2 \cdot 8H_2O$
5	7.59	4.47	313.15	$LiBO_2 \cdot 2H_2O$
6	8.09	4.47	323.15	$LiBO_2 \cdot 2H_2O$
7	4.66	10.31	303.15	$LiBO_2 \cdot 8H_2O$
8	7.23	10.31	313.15	$LiBO_2 \cdot 2H_2O$
9	7.46	10.31	323.15	$LiBO_2 \cdot 2H_2O$

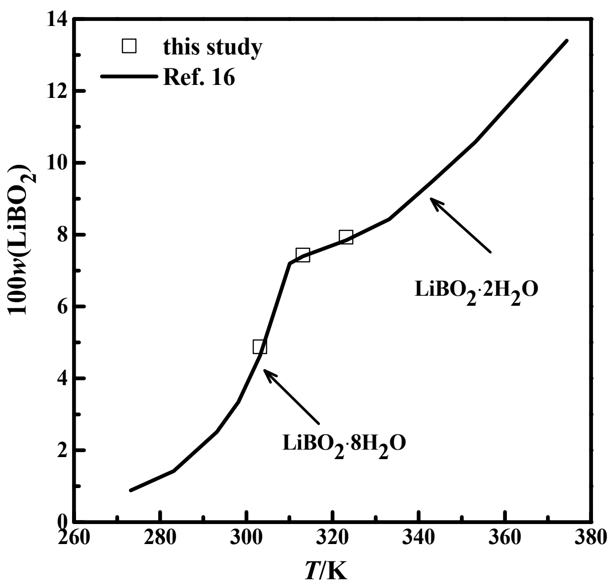

Figure 2. Comparison of the solubility of $LiBO_2$ in this study with literature data: —, [16]; □, this study.

The XRD patterns of the solid phase in the systems $LiBO_2-H_2O$ and $LiBO_2-NaCl-H_2O$ at different temperatures were shown in Figure 3. The XRD spectrogram was analyzed with the software MDI Jade (Jade 6.0, Materials Date, Inc. Livermore, CA, USA). The characteristic peak of the samples agree with those of $LiBO_2{\cdot}2H_2O$ and $LiBO_2{\cdot}8H_2O$ in Figure 3. Therefore, it can be judged that the solid phase is $LiBO_2{\cdot}2H_2O$ or $LiBO_2{\cdot}8H_2O$. From Figure 3, the corresponding equilibrium salts for the saturated solution at 313.15 K and 323.15 K is $LiBO_2{\cdot}2H_2O$, and at 303.15, it is $LiBO_2{\cdot}8H_2O$. From Table 1, the solubility for lithium chloride salts in NaCl solution is bigger than that in pure solution when the concentration of NaCl is 0.0447 (mass fraction), while being smaller when the concentration of NaCl is 0.1031. In general, the solubility data for $LiBO_2{\cdot}2H_2O$ was similar in the presence of NaCl at various concentrations.

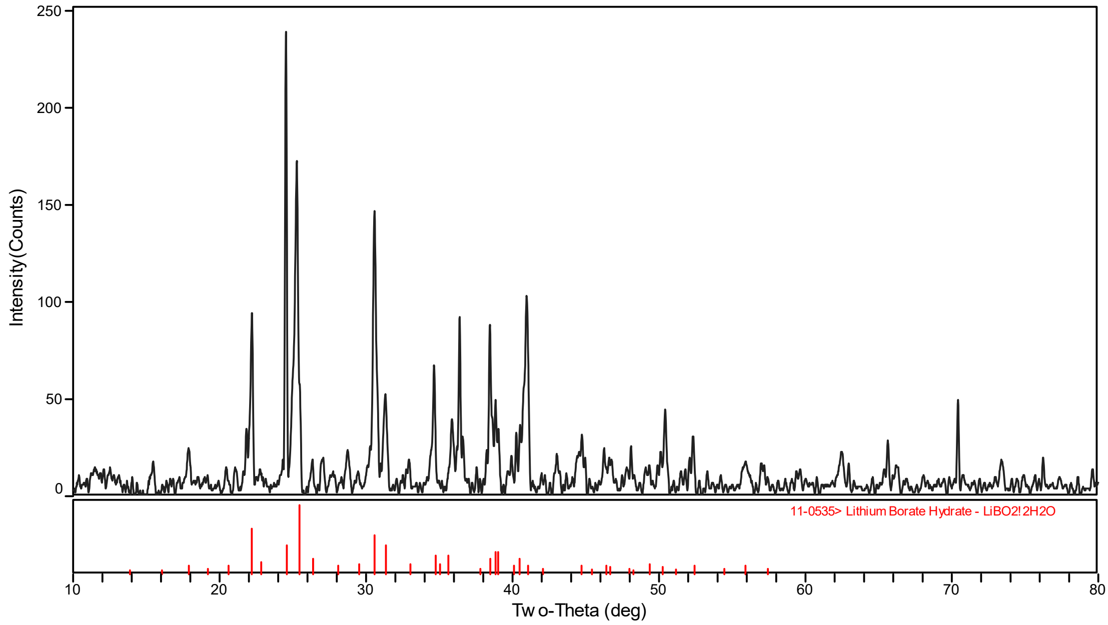

(**a**)

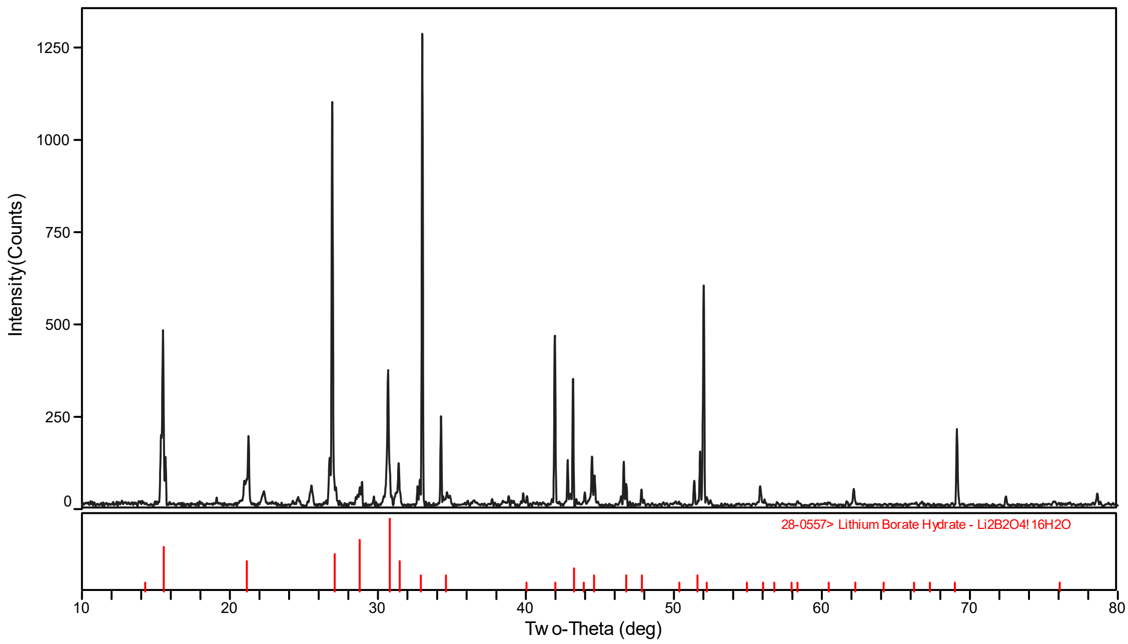

(**b**)

Figure 3. XRD pattern for (**a**) $LiBO_2{\cdot}2H_2O$ and (**b**) $LiBO_2{\cdot}8H_2O$.

3.2. Metastable Zone Width in Lithium Metaborate Solutions

According to classical nucleation theory, adequate mechanical energy can be obtained from the solution with the improvement of stirring strength. In addition, it will lead to the intensification of the collision between the magnetic stirring rotator, the solute, and the mold wall, which will increase the probability of collision nucleating agents. Meanwhile, the increase of the heat transfer rate is beneficial to the timely diffusion of heat generated by crystalline phase transformation [7]. The MZW of lithium metaborate salts with different stirring rates at cooling rates of 12.0 $K \cdot h^{-1}$ are tabulated in Table 2. The MZW of lithium metaborate salts decreased when the stirring rate increasing. In order to stabilize the crystallization process, the stirring rate of 200 r/min is selected.

Table 2. Lithium metaborate with different stir rates.

$100w(LiBO_2)$	$\triangle T_{max}$/K		
	100 r/min	200 r/min	400 r/min
4.88	12.92	11.11	11.86
7.43	19.00	17.24	17.68
7.93	28.13	26.70	25.81

The MZW was obtained at various cooling rates and solutions with no impurity. The MZW data with a constant stirring rate 200 r/min are summarized in Table 3. It is noted that the temperature for lithium metaborate salts precipitated from different saturated solutions (from 303.15 K to 323.15 K), which are all below 303.15 K. The lithium metaborate salts precipitated from different saturated solutions are the same salt $LiBO_2 \cdot 8H_2O$, which were indentified using XRD. From Table 3, the MZW increases as the increasing concentration of lithium metaborate or cooling rate, which is similar to that of boric acid as well as phosphoric acid and sodium tetraborate decahydrate [8,17], but inverse of the oxalic acid in the water system [18].

Table 3. Width of lithium metaborate salts with different cooling rates and a different impurity concentration.

$100w(NaCl)$	$100w(LiBO_2)$	$\triangle T_{max}$ (K)			
		6 K/h	9 K/h	12 K/h	18 K/h
0.00	4.88	9.13	10.82	11.11	13.24
	7.43	14.99	16.44	17.24	19.16
	7.93	22.61	25.06	26.70	28.67
4.47	4.97	14.77	16.27	16.98	19.10
	7.59	20.69	22.16	24.29	24.85
	8.09	28.14	30.44	31.38	32.83
10.31	4.66	20.00	21.45	22.52	25.09
	7.23	26.76	27.87	29.55	31.34
	7.46	33.13	35.92	38.13	39.68

3.3. Impurities on the MZW for Lithium Metaborate Solutions

The effect of NaCl impurity on the MZW of lithium metaborate was studied in the temperature range from 303.15 K to 323.15 K. Various cooling rates were investigated to measure the MZW of lithium metaborate salts with various sodium chloride concentrations. The MZW of lithium metaborate salts was also tabulated in Table 3. In Table 3, there is a noticeable increase of the MZW for lithium metaborate salts with increasing cooling rates and concentration of sodium chloride, which is similar to that of $Na_2B_4O_7 \cdot 10H_2O$ with KCl impurity [11].

The enlargement effect of impurities on MZW can be possibly interpreted that, with the impurity, molecules are absorbed on the surface of subcritical embryos in the solution [12]. Therefore, those impurities hinder the embryos growing larger than the critical size and lead to the enlargement of the MZW.

3.4. Apparent Nucleation Order of Lithium Metaborate Solutions

The relationship between MZW and the cooling rate have already been reported in past studies. The Nývlt's approach is widely applied for the MZW research [19,20]. The following expressions are the main equations in the Nývlt's approach.

$$\log \Delta T_{max} = \frac{1-m}{m} \log\left(\frac{\mathrm{d}W_{eq}}{\mathrm{d}T}\right) - \frac{\log \mathrm{K_N}}{m} + \frac{1}{m}\log(-b) \tag{2}$$

where $-b$ is the constant cooling rate (K/h) and $\mathrm{K_N}$ denotes the nucleation rate constant. $\mathrm{d}W_{eq}/\mathrm{d}T$ is the solubility dependence on the temperature change. $\log\Delta T_{\max}$ and $\log(-b)$ has a linear relationship in Equation (2). Therefore, it can be replaced by Equation (3).

$$y = A + Bx \tag{3}$$

where x is $\log(-b)$ and y is $\log\Delta T_{\max}$. The apparent secondary nucleation order m can be calculated with Equations (3) and (4).

$$m = 1/B \tag{4}$$

From the MZW of lithium metaborate salts, the relationship between $\log\Delta T_{max}$ and $\log(-T)$ were presented in Figure 4. The coefficients A, B, and m were obtained with the linear result analysis, as shown in Table 4. The nucleation order m of lithium metaborate salts with NaCl impurity is larger than that in pure solution. This result illustrates that a higher m of lithium metaborate salts can be obtained when the NaCl impurity is added.

Table 4. Apparent order m of lithium metaborate salts in the solution containing sodium chloride.

$100w$(NaCl)	$100w(\mathrm{LiBO_2})$	Nucleation Equation	R^2	m
0.00	7.93	$y = 1.1893 + 0.2164x$	0.9876	4.62
	7.43	$y = 1.0043 + 0.2196x$	0.9915	4.55
	4.88	$y = 0.7129 + 0.3222x$	0.9469	3.10
4.47	8.09	$y = 1.3460 + 0.1381x$	0.9614	7.24
	7.59	$y = 1.1810 + 0.1765x$	0.9008	5.67
	4.97	$y = 0.9906 + 0.2285x$	0.9827	4.38
10.31	7.46	$y = 1.3941 + 0.1670x$	0.9600	5.99
	7.23	$y = 1.310 + 0.1476x$	0.9769	6.78
	4.66	$y = 1.1397 + 0.2040x$	0.9771	4.90

From Figure 4, the lines are not fully parallel because of various experimental errors. Thus, the lines were modified using an improved linear regression method [19]. The coefficient B were calculated with Equation (5).

$$B = \frac{\sum\limits_{j=1}^{p} [\sum\limits_{i} x_i y_i - \sum\limits_{i} x_i / N_j \times \sum\limits_{i} y_i]_j}{\sum\limits_{j=1}^{p} [\sum\limits_{i} x_i^2 - (\sum\limits_{i} x_i)^2 / N_j]_j} \tag{5}$$

where p represents the total number of lines, i is the number of the cooling rate, and N_j is the number of experiments for line j.

For MZW data using the laser technique in the pure system $\mathrm{LiBO_2{-}H_2O}$, B calculated from Equation (5) is 0.2503, and m of lithium metaborate salts is 4.00. The presence of NaCl impurity enlarged the apparent secondary nucleation order. With w(NaCl) = 0.447 in the solution, the m of lithium metaborate salts is 5.44, and 5.67 with w(NaCl) = 0.1031 in the solution. The m of lithium metaborate salts increased with increasing w(NaCl).

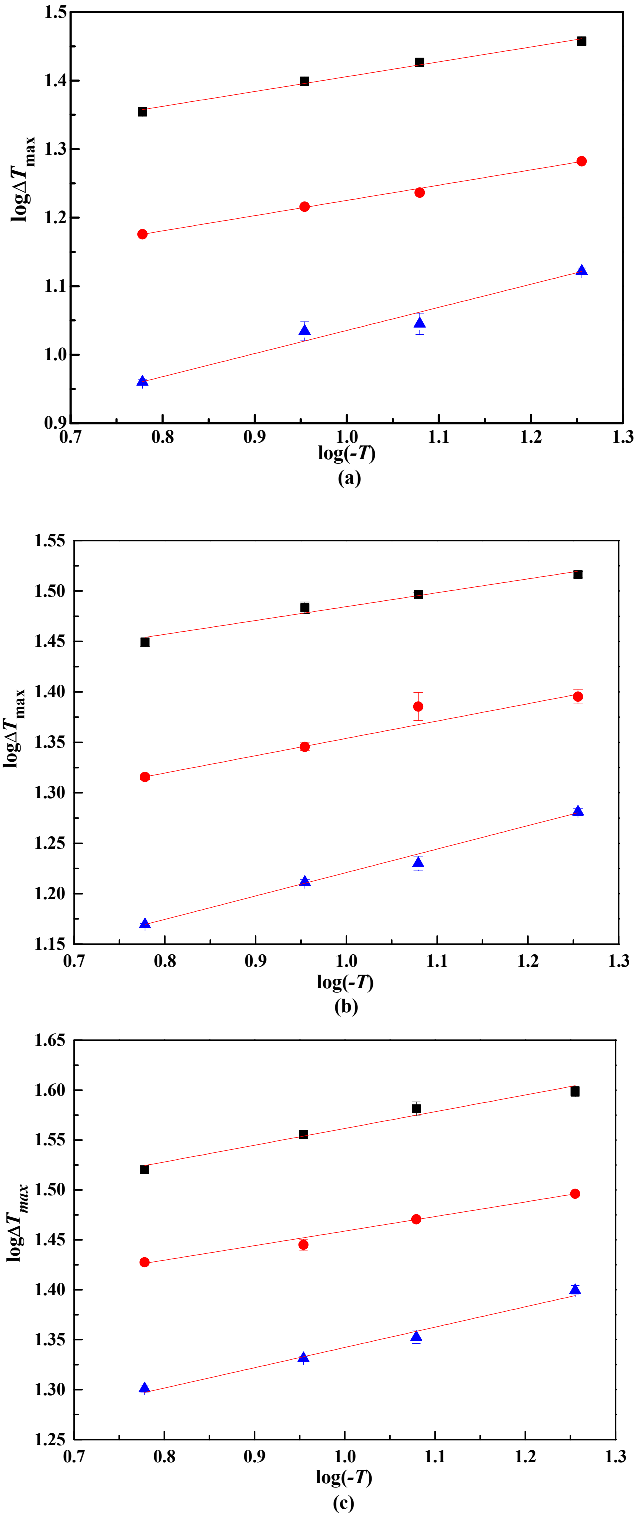

Figure 4. log ΔT_{max} and log($-T$) in NaCl solutions. ■, 323.15 K. ●, 313.15 K.▲, 303.15 K. NaCl (100w): (**a**), 0.00. (**b**), 4.47. (**c**): 10.31.

4. Conclusions

The solubilities of lithium metaborate salts at different temperatures in pure and sodium chloride solution were obtained with the isothermal equilibrium method. The solubility data for lithium metaborate salts was virtually unchanged in the presence of NaCl impurities at various concentrations. The metastable zone width of lithium metaborate salts at various concentrations was determined using the laser technique. The MZW of lithium metaborate salts decreased when the stirring rate increased, but increased remarkably with increasing cooling rates and an increasing concentration of sodium chloride. The Nývlt's approach was applied to calculate the secondary nucleation order m for lithium metaborate salts. The m of lithium metaborate salts is 4.00 in a pure $LiBO_2-H_2O$ system with an improved linear regression method. The m for lithium metaborate salts was enlarged in system $LiBO_2-NaCl-H_2O$. The results can provide a theoretical direction and important data for the comprehensive development of lithium metaborate salts from brine.

Author Contributions: D.L., Y.M., and L.M. conceived and designed the experiments. D.L. and Y.M. performed the experiments. L.Y. analyzed the data. All authors wrote the paper.

Funding: The National Natural Science Foundation of China (U1607123 and 21773170), the Foundation of Tianjin Key Laboratory of Marine Resources and Chemistry (Tianjin University of Science & Technology) (2018-04), and the Yangtze Scholars and Innovative Research Team of the Chinese University (IRT_17R81) jointly funded this work.

Conflicts of Interest: The authors declare no conflict of interest.

References

1. Gao, S.Y.; Song, P.S.; Zheng, M.P.; Xia, S.P. *Salt Lake Chemicals*; Science Press: Beijing, China, 2007.
2. Gao, S.Y.; Li, G.Y. The chemistry of borate in salt lake brine (I) behavior of borate during solar evaporation of brine. *Chem. J. Chin. Univ.* **1982**, *3*, 141–148.
3. Gao, S.Y.; Fu, T.J.; Wang, J.Z. Chemistry of borate in salt lake brine III. maximum solubility of mg-borate in concentrated salt lake brine. *Chin. J. Inorg. Chem.* **1985**, *1*, 97–102.
4. Meng, L.Z.; Guo, Y.F.; Li, D.; Deng, T.L. Solid and liquid metastable phase equilibria in the aqueous quaternary system Li^+, $Mg^{2+}//SO_4^{2-}$, Borate-H_2O at 273.15 K. *Chem. Res. Chin. Univ.* **2017**, *33*, 655–659. [CrossRef]
5. Gurbuz, H.; Ozdemir, B. Experimental determination of the metastable zone width of borax decahydrate by ultrasonic velocity measurement. *J. Cryst. Growth* **2003**, *252*, 343–349. [CrossRef]
6. Sun, Y.Z.; Song, X.F.; Wang, J.; Luo, Y.; Yu, J. Unseeded supersolubility of lithium carbonate: Experimental measurement and simulation with mathematical models. *J. Cryst. Growth* **2009**, *311*, 4714–4719. [CrossRef]
7. Wang, P.P.; Yu, P.B.; Wu, Q.F.; Chen, J.X. Determination of freezing eutectic crystallization metastable zone of monosodium glutamate. *Chem. Eng.* **2017**, *45*, 33–36. [CrossRef]
8. Sayan, P.; Ulrich, J. Effect of various impurities on the metastable zone width of boric acid. *Cryst. Res. Technol.* **2001**, *36*, 411–417. [CrossRef]
9. Meng, Q.F.; Dong, Y.P.; Kong, F.Z.; Feng, H.T.; Li, W. Study on the metastable zone property of boric acid in different concentrations of $MgCl_2$ and NaCl solutions. *Acta Chim. Sinica* **2010**, *68*, 1699–1706.
10. Kong, F.Z.; Dong, Y.P.; Meng, Q.F.; Peng, J.Y.; Li, W. Study of the metastable zone property of H_3BO_3 in $CaCl_2$–H_3BO_3–H_2O system. *J. Salt Lake Res.* **2011**, *19*, 48–53.
11. Peng, J.Y.; Dong, Y.P.; Nie, Z.; Kong, F.Z.; Meng, Q.F.; Li, W. Solubility and metastable zone width measurement of borax decahydrate in potassium chloride solution. *J. Chem. Eng. Data* **2012**, *57*, 890–895. [CrossRef]
12. Peng, J.Y.; Dong, Y.P.; Wang, L.P.; Li, L.L.; Li, W.; Feng, H.T. Effect of impurities on the solubility, metastable zone width, and nucleation kinetics of borax decahydrate. *Ind. Eng. Chem. Res.* **2014**, *53*, 12170–12178. [CrossRef]
13. Sahin, O.; Dolas, H.; Demir, H. Determination of nucleation kinetics of potassium tetraborate tetrahydrate. *Cryst. Res. Technol.* **2007**, *42*, 766–772. [CrossRef]

14. Li, D.; Meng, L.Z.; Guo, Y.F.; Deng, T.L.; Yang, L. Chemical engineering process simulation of brines using phase diagram and Pitzer model of the system $CaCl_2-SrCl_2-H_2O$. *Fluid Phase Equilibr.* **2019**, *484*, 232–238. [CrossRef]
15. Qinghai Institute of Salt Lakes, Chinese Academy of Science. *Analytical Methods of Brines and Salts*, 2nd ed.; China Science Press: Beijing, China, 1988.
16. Reburn, W.T.; Gale, W.A. The system lithium oxide−boric oxide−water. *J. Phys. Chem.* **1955**, *59*, 19–24. [CrossRef]
17. Ma, Y.; Wang, Z.; Zhou, J.Y. Effects of impurity ions on the metastable zone width of phosphoric acid in tributyl phosphate. *J. Chem. Eng. Data.* **2014**, *59*, 2909–2913. [CrossRef]
18. Omar, W.; Ulrich, J. Solid liquid equilibrium, metastable zone, and nucleation parameters of the oxalic acid-water system. *Cryst. Growth. Des.* **2006**, *6*, 1927–1930. [CrossRef]
19. Nývlt, J.; Söhnel, O.; Matuchová, M.; Broul, M. *The Kinetics of Industrial Crystallization*; Elsevier: Amsterdam, The Netherlands, 1985.
20. Mullin, J.W. *Crystallization*, 4th ed.; Butterworth-Heinemann: London, UK, 2001.